

# THE JOURNAL OF PHYSICAL CHEMISTRY C

A JOURNAL OF THE AMERICAN CHEMICAL SOCIETY

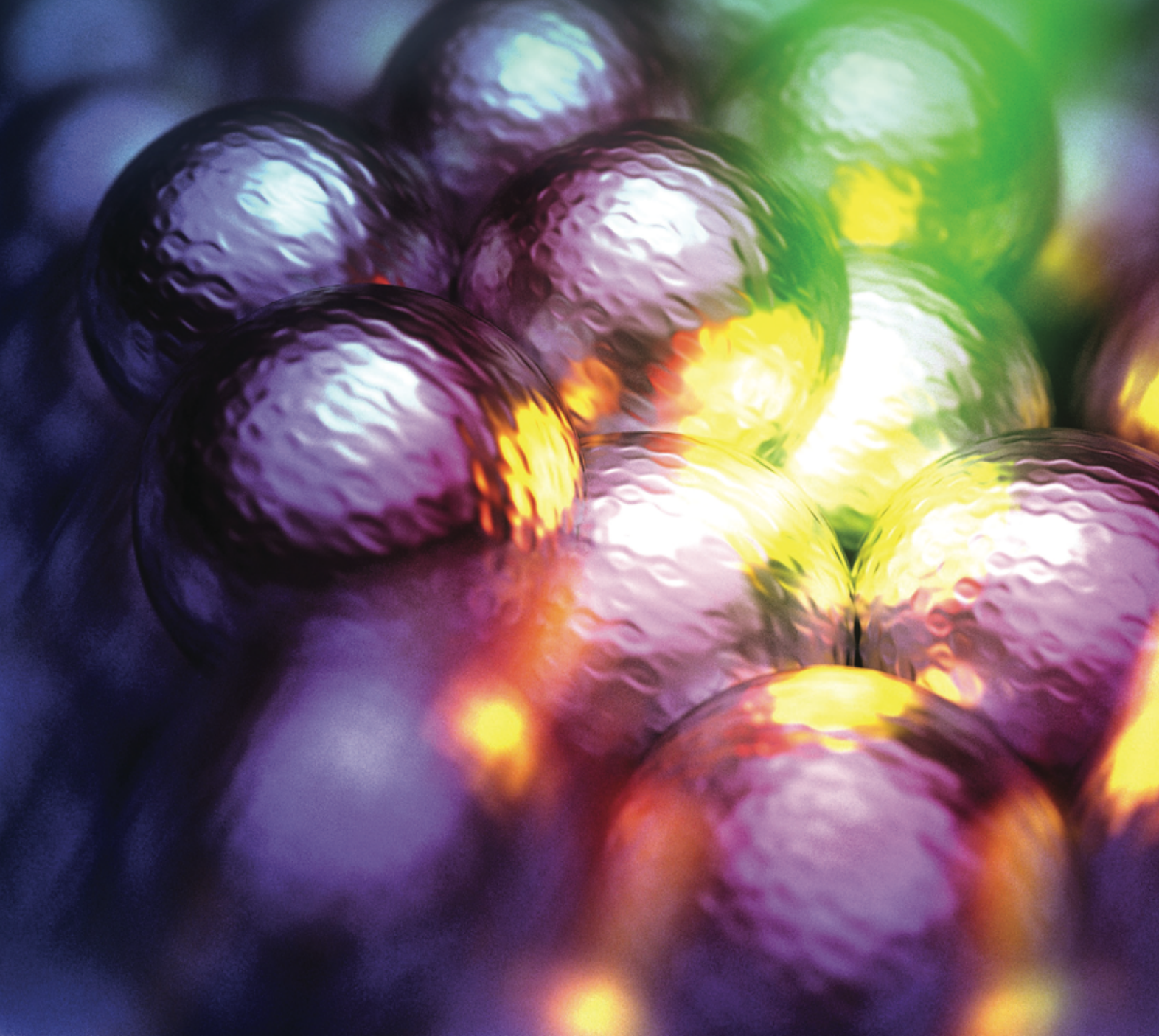


April 15, 2021

Volume 125

Number 14

[pubs.acs.org/JPCC](https://pubs.acs.org/JPCC)



ACS Publications  
Most Trusted. Most Cited. Most Read.

[www.acs.org](https://www.acs.org)

# Ultra-High-Speed Dynamics in Surface-Enhanced Raman Scattering

Nathan C. Lindquist and Alexandre G. Brolo\*



Cite This: <https://dx.doi.org/10.1021/acs.jpcc.0c11150>



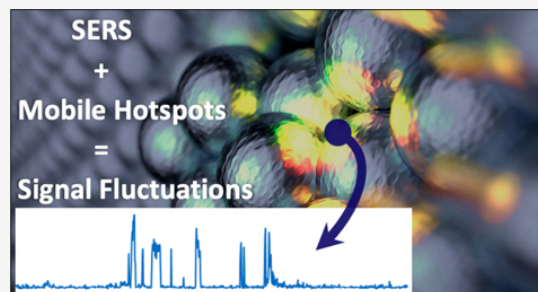
Read Online

ACCESS |

Metrics & More

Article Recommendations

**ABSTRACT:** In this perspective, we discuss recent observations related to the temporal dynamics of intensities in surface-enhanced Raman scattering (SERS) experiments. SERS is a well-established and highly active research field, driven by the potential of the technique in analytical and bioanalytical applications. However, there are several fundamental aspects of the effect that still challenge and fascinate researchers in the area. Here we will focus on the recent observation that strong SERS intensity fluctuations (SIFs) are seen when experiments are performed at fast acquisition rates, even when the metal surface is completely covered by an adsorbate. Interestingly, the SIF dynamics indicate bursts of SERS activities that last only a few hundreds of microseconds, followed by a longer period of inactivity. This type of behavior has been observed from several systems and configurations, including single metallic nanoshells and nanostars, immobilized colloidal aggregates, nanoparticle-on-a-mirror configurations, and metal-coated microspheres. This diversity suggests that the dynamical behavior is a fundamental characteristic of the SERS effect. Time-dependent atomic rearrangements within the confined environment of the SERS hotspots are suggested as the main mechanism driving these fluctuations. The dynamical SERS behavior, revealed with high-speed acquisitions, should provide a new direction for the study of atomic reconstruction and single molecule interactions with metallic nanoenvironments with an unprecedented level of detail.



## INTRODUCTION

The surface-enhanced Raman scattering (SERS) effect represents well the power, potential, and fundamental challenges related to both nanotechnology and nanophotonics.<sup>1</sup> SERS is the large enhancement in Raman scattering observed from molecules that are in regions of concentrated electric fields present in metallic nanostructures. These highly localized electric fields, known as SERS “hotspots”, are created by the excitation of surface plasmon resonances, and they depend heavily on the geometric parameters of the nano-environment.<sup>2</sup> SERS adds exquisite single-molecule sensitivity to the typical fingerprinting capabilities of vibrational Raman spectroscopy, creating a broad range of opportunities in analytical chemistry.<sup>3,4</sup> The potential applications of SERS largely drives research and interest in the field, but there are several fundamental aspects of the phenomenon that still fascinate and perplex researchers in the area.<sup>5</sup> Among those fundamental aspects are time-series fluctuations in both SERS intensities and spectral characteristics that are ubiquitous to the effect.<sup>6–8</sup> SERS intensity fluctuations (SIFs) have been reported mainly in the context of single-molecule detection by SERS (single-molecule surface-enhanced spectroscopy, SM-SERS). Early reports of SM-SERS suggested that SIFs were observed only in experiments at very low concentrations (<100 nM), since in those conditions just one molecule would be, on average, present under the laser illuminated area at a given time.<sup>9</sup> Similarly, for experiments in liquid suspension, just one

nanoparticle would be illuminated. This type of reasoning is standard in single-molecule fluorescence spectroscopy.<sup>10</sup> However, several reports of SIF behavior challenged this simple analogy with single-molecule fluorescence. These include experiments involving dry samples<sup>11</sup> and single nanostructures<sup>12</sup> with surface concentrations much higher than would permit only a single molecule to be illuminated at a time.<sup>13</sup> It was also established that SIF behavior can be both temporally and spatially dependent, with significant differences in SERS activity within regions that are only a few nanometers apart. All of these results suggest that the light/matter interactions as it relates to SERS should be reimagined by considering that the nanoparticle surface, the adsorbed molecules, and the plasmonic hotspots form a dynamical environment, where even atomic-scale effects come into play. Recently, a new class of extremely short-lived SIFs have been unveiled from SERS experiments done with high data acquisition rates.<sup>14</sup> These new ultrahigh speed time-dependent SIFs were revealed using SERS acquisition rates approaching 1 million samples per second, much larger than the typical 1 s

Received: December 14, 2020

Revised: February 20, 2021

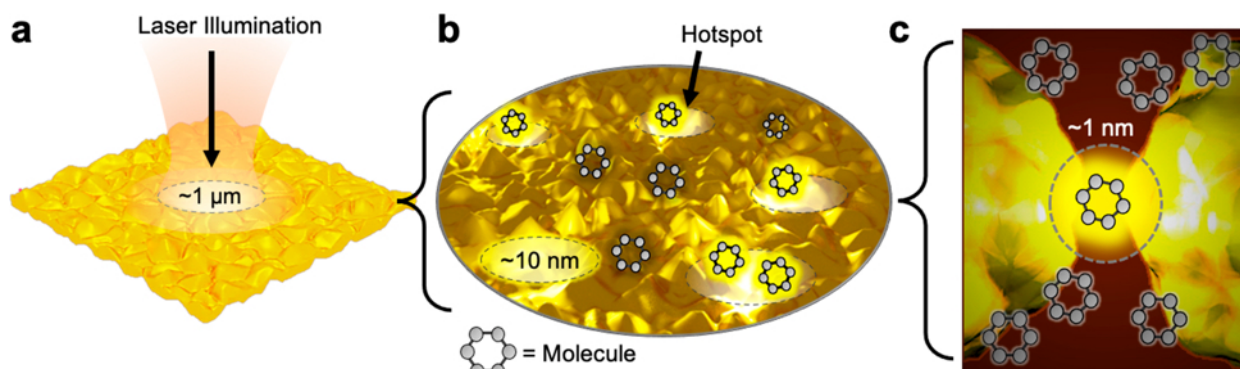


**Figure 1.** Schematic representation of the electric field distribution at nanostructured surfaces under different conditions and length scales. (a) A nanostructured surface is illuminated by a  $\sim 1 \mu\text{m}$  diameter laser excitation. (b) Within the 10s of nm length scale, the local field is distributed spatially, generating regions of high intensity (hotspots). At low surface concentrations, the probability of a single molecule finding a hotspot dictates the fluctuating behavior of the SERS intensities. (c) In certain situations, such as in nanoparticle dimers, a nanoparticle-on-a-mirror (NPoM) configuration, or a scanning near-field probe tip, the field can be tightly localized in a single “atomic” hotspot (pico-cavity), allowing single molecule measurements even from a fully coated surface.

acquisition time used in regular SERS measurements. The newly revealed high-speed SIF dynamics should carry fundamental information related to time-sensitive processes in a molecule/hotspot environment. Here we will discuss the fundamentals of this phenomenon and its implications, including the relationship to several other recent advances in plasmon-induced enhanced Raman effects.

## ■ A BRIEF DESCRIPTION OF TIME-DEPENDENT SERS INTENSITY FLUCTUATIONS (SIFs)

The concept of plasmonic hotspots is central to interpreting the SERS effect and provides an understanding of SIFs in the context of a purely electromagnetic enhancement mechanism.<sup>6</sup> It is also widely accepted that “chemical mechanisms” and resonance Raman effects<sup>15</sup> also play a role in enhancing the Raman response from adsorbed molecules.<sup>16,17</sup> In fact, there are even reports of highly sensitive “SERS” from nonplasmonic structures.<sup>18,19</sup> In those cases, the enhancement is driven by resonances that involve new electronic transitions available in the nanoenvironment. While chemical and molecular resonance mechanisms can be extremely relevant for certain systems,<sup>15</sup> here we will restrict the discussion to plasmonic and hotspot-driven SERS, since it provides the bulk of the enhancement in a typical experiment with noble metal nanostructures.

In order to help understand the basic features of SIFs, we will consider a random metallic nanostructured surface as a SERS substrate illuminated by a focused laser beam. A schematic of the main features of this generic model is illustrated in Figure 1. The substrate in Figure 1 can be a representation of, for example, a roughened silver electrode or a set of gold nanoparticles aggregated on a glass slide. The archetypical plasmonic SERS hotspot is generated by a metallic nanoparticle dimer that concentrates electric field at its junction.<sup>20</sup> Other geometric features, such as single protrusions, roughness structures, crevices, and gaps also enable field localization.<sup>21</sup> The rough surface in Figure 1 contains a distribution of these nanometric features with different geometries, generating hotspots of different strengths within the laser illuminated area. Notice that this distribution of hotspots might even occur within a single nanoparticle, or for any fabricated nanostructure, due to the presence of surface roughness and defects. The important realization in this model

is that the plasmonic hotspots, illustrated in Figure 1b, are highly localized and on deeply subwavelength scales. This means that, although the laser spot in Figure 1a is  $\sim 1 \mu\text{m}$  in diameter, the enhanced Raman signal will be generated mostly within the few square nanometers of the hotspot regions.<sup>22</sup> In fact, it has been established that only a small fraction of the adsorbed molecules ( $\sim 1\%$ ) in a fully coated surface will contribute to the majority of the SERS response over a large area.<sup>23</sup> Moreover the electric field at the hotspot is strongest at the surface and decays away toward the dielectric environment with typical decay lengths of just a few tens of nanometers.<sup>20–22</sup> In contrast to fluorescence, where the laser illumination defines the probing volume, in SERS the volume and strength of the field distribution within each hotspot will dictate the contribution of the various molecules to the overall detected signal. Highly efficient hotspots, capable of generating a measurable SERS signal from just a single molecule, are rare. Consequently, even when the amount of molecules under the laser illuminated area is, on average, much larger than one, there is still the probability of observing SM-SERS events that originate from the occasional and intermittent case when a single molecule, by chance, finds a very strong hotspot (Figure 1b). The detected signal in this case will depend on the ability of the molecule/hotspot system to generate enough photons to surpass the detection threshold given by the noise level and sampling conditions of the experimental system. This is an interesting experimental challenge since it suggests that the characteristics of SM-SERS would be perceived differently in different instruments. For instance, only Raman scattering from very strong hotspots would contribute to the detectable signal when a low collection efficiency microscope is used. Likewise, only long time-scale effects will be observed, and high-speed effects will be averaged out by a slow data acquisition rate.

The situation illustrated in Figure 1 shows that, even at relatively low surface concentrations, several molecules can be directly illuminated by the laser yet *not* be “illuminated” by a much smaller hotspot. The whole SERS signal, therefore, will reflect the contribution of a single molecule that found a rare hotspot by chance as well as any other background contributions. Figure 1c shows a situation that is becoming more common in recent years, where SIFs are observed from surfaces completely covered by a probe molecule. This is

possible when there is only one highly localized strong hotspot that dominates the response of the system at a particular time. This condition has been encountered in different types of configurations, such as in tip-enhanced Raman scattering (TERS),<sup>24</sup> in a nanoparticle-on-a-mirror (NPoM) geometry,<sup>25,26</sup> and in single particle SERS.<sup>14</sup> The highly confined field is related to pico-cavities formed due to atomic protrusions. The mechanism that drives these atomic reconstruction processes is still being investigated, although preliminary results point toward a thermally activated path.<sup>14,25</sup> It is important to emphasize that in all these situations the excitation laser illuminates a large number of molecules, but just a few (ultimately just one) in a very localized region of a unique hotspot will contribute to the SERS response. This single molecule condition has been verified through experiments using isotopologues.<sup>27</sup>

The relationship between the strength and density of hotspots and the number of molecules at the surface affect the frequency and the relative intensity of the SIFs. Histograms of SERS intensities will follow different distributions, depending on those parameters.<sup>28,29</sup> This is illustrated by the histograms<sup>28</sup> presented in Figure 2. Figure 2a shows that at

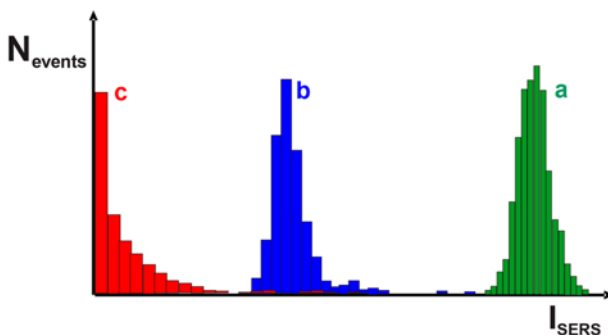


**Figure 2.** Examples of typical distributions of SERS intensities. The histograms are for rhodamine 6G (R6G) adsorbed on a nanostructured silver surface at different concentrations.<sup>28</sup> For clarity, the histograms were shifted along the  $x$ -axis ( $I_{\text{SERS}}$ ) to avoid superimposing each other. (a) In a “high concentration” regime,  $[R6G] = 5 \mu\text{M}$ , the SERS signal does not vary much with time and the distribution follows a normal behavior. (b) As the concentration decreases,  $[R6G] = 100 \text{ nM}$ , a few highly efficient hotspots start to contribute more to the overall signal and the dynamics of molecules visiting those hotspots are manifested by adding an asymmetry (tail toward higher intensities) to the distribution. (c) At very low concentrations (ultimately at the single molecule regime), here  $[R6G] = 10 \text{ nM}$ , a power-law probability distribution emerges. In this case, most of the time-dependent events yield little if any signal, but some events provide a SERS spectrum indicating that a single molecule visited a hotspot.

high surface concentrations and/or a large number of hotspots, the temporal (or spatial) dependence of SERS intensities variations will be small and the SERS intensity distribution should follow a narrow Gaussian function. Of course, additional variations due to time-dependent photodegradation and other photochemical and thermal effects could also play a role,<sup>30</sup> but we are only focused on the ideal situation in this example. This type of distribution is useful for analytical applications, since the average intensity in this case can be correlated to the concentration of the species in solution. As the surface concentration decreases, the width of the Gaussian distribution broadens (larger standard deviation). This occurs

because a smaller number of molecules to number of hotspots ratio affects the standard deviation. Eventually, as shown in Figure 2b, the Gaussian shape morphs to a log-normal distribution. The tail toward high intensity values in the asymmetric log-normal distribution emphasizes the fact that just a very small number of molecules will actually be able to access the most efficient hotspot areas. We should remember that hotspots are not uniform, and even in a case where all of them have the same strength (defined as the maximum enhancement factor in ref 29), still only a very small region of the total surface area will contribute to the overall SERS signal. A continuous decrease in surface concentration emphasizes the characteristic tail of the distribution and shifts the average intensity to lower values. For very low concentrations, when the amount of molecules inside the illuminated area is very small relative to the density of hotspots, the SIFs will become more severe. Most of the spectra (recorded, for instance in a time dependent series) will just display noise, with only a few events showing high SERS response. A typical distribution of SERS intensities in this low concentration limit case is represented in Figure 2c. Ultimately, the single molecule regime is achieved, meaning that each event that produces a momentary SERS signal is most likely generated by an individual molecule visiting a particular hotspot.<sup>6</sup> In that case, the tailed distribution, such as the one in Figure 2c, reflects the distribution of hotspot strengths, since every single molecule event produces an intensity related to the enhancement characteristics of the hotspot visited by the molecule.<sup>31</sup> A tailed distribution of SERS intensities (Figure 2c) can be observed even for high surface concentrations. An extreme example is the limit where there is only one hotspot (for instance in NPoM experiments<sup>32</sup>), where the tight light localization allows for just one molecule to be probed, as represented earlier in Figure 1c.

## ULTRAHIGH SPEED SERS

The discussion of Figures 1 and 2 presents a classical view to rationalize the SIFs. In those cases, the main constraints are the spatial localization of the light field and the surface concentration. The nature of the dynamical processes that actually drives the time-dependence of the fluctuations were not emphasized. Among the several potential mechanisms, molecular adsorption equilibrium has been suggested to account for the situation described in Figure 1b. These adsorption/desorption processes can be dominant for experiments realized in solutions, while molecular surface diffusion could play a significant role for experiments using dry samples. The intensity fluctuations in the conditions described in Figure 1c are different. In that case, if the surface is completely covered, molecular movement would be restricted. However, SM-SERS can still be observed due to the high degree of field localization inside the cavity. This situation can be observed in different systems, such as nanoparticle dimers, TERS and NPoM. Recent results involving TERS<sup>24</sup> and NPoM<sup>25</sup> configurations suggest that the fluctuations in those cases are driven by a transient increase in the local hotspot strength due to atomic reconstruction.<sup>11,25</sup> In other words, a single hotspot “finds” a molecule instead of the molecule finding the hotspot. This is a new concept in SERS and contrasts with the view of a static distribution of hotspots over the surface. These results suggest that, beyond the molecular mechanisms of adsorption, desorption and diffusion, intrinsic dynamics related to atomic metal elements at the hotspot induces a fast dynamic of

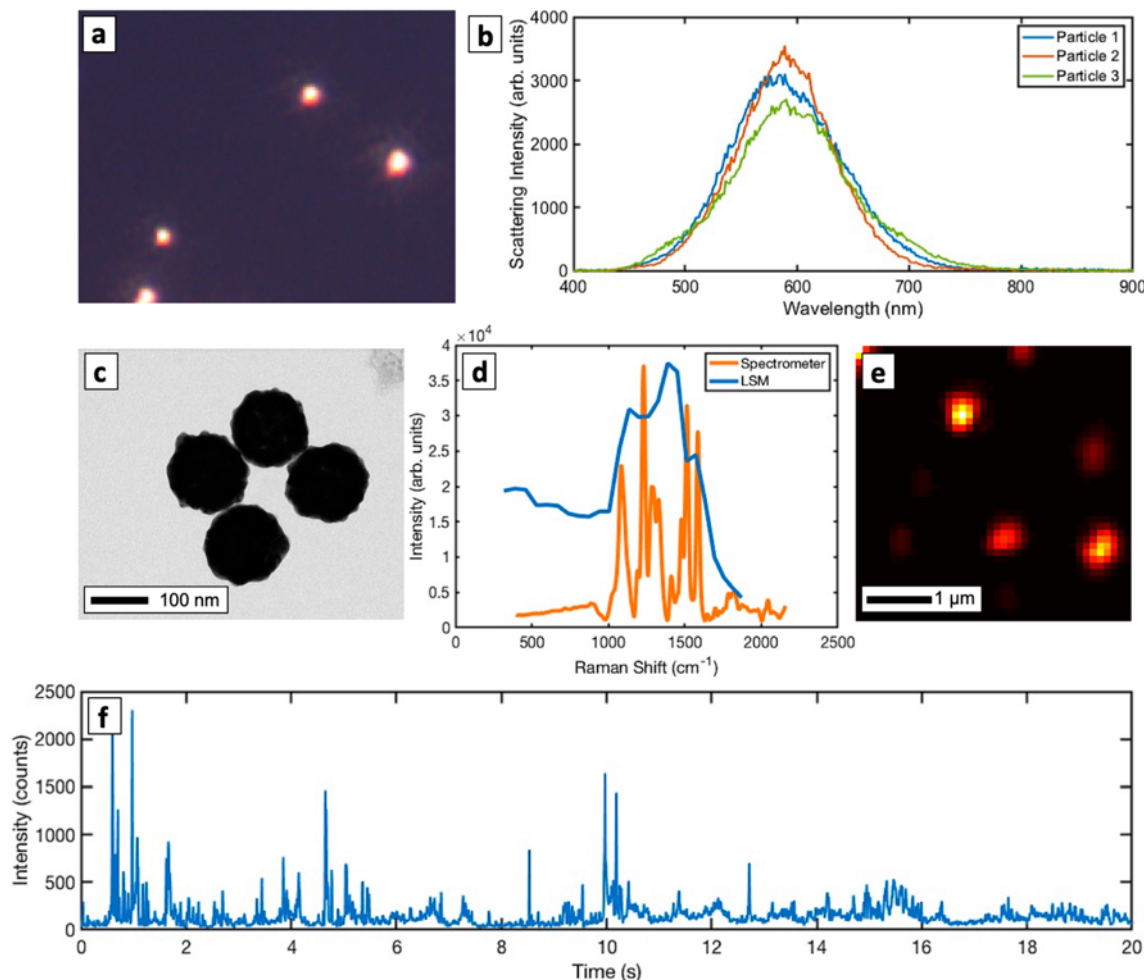


**Figure 3.** SIF events from single nanoparticles with a laser scanning microscope (LSM). The single nanoparticles were  $\sim 100$  nm silver nanoshells<sup>36</sup> fully coated with a self-assembled monolayer of 5,5'-dithiobis(2-nitrobenzoic acid) (DTNB). (a) Dark-field microscopy image of nanoshells immobilized in a glass slide. (b) Sample scattering spectra from three nanoshells. The nanoshells are tuned to have an LSPR in the visible and accessible with red and green lasers. (c) TEM image of the nanoshells used in this study. (d) SERS spectra obtained using scanning bandpass filters and from a standard Raman microscope equipped with a high-resolution spectrometer. (e) SERS intensity image (bandpass filter set to collect the entire  $1000\text{--}1600\text{ cm}^{-1}$  Stokes-shifted region) from the laser scanning microscope and the  $633\text{ nm}$  laser. (f) Plots of a single point SERS intensity trajectory from one of the nanoshells shown in panel e. Figure adapted with permission from ref 13. Copyright 2020 American Chemical Society.

intensity and spectral fluctuations that are present in a variety of SERS (and related phenomenon, such as TERS) systems.

The effect of fast acquisition time on the intensity fluctuations in SERS has not been widely explored yet, but it can provide information on the relative importance of various processes that contribute to the effect.<sup>33</sup> As the acquisition time is decreased, only molecules in very efficient hotspots regions will be able to produce enough photons to overcome the signal-to-noise ratio (*S/N*) threshold of the acquisition system. Therefore, the shape of the distribution of SERS intensities should behave as in Figure 2c, but with a fixed concentration and different acquisition rates. In the limit of very fast acquisition, on the submicrosecond time scale, the condition for a very small number of molecules contributing to the signal is reached even if the surface is completely covered. This realization adds a new dimension to SERS, since it allows probing fast dynamic events at highly efficient hotspots at the single molecule level even from a fully coated surface by using ultrahigh speed acquisition rates ( $\sim 1$  MHz). However, most of the instrumentation used for SERS experiments is equipped with CCD detectors and equivalent cameras, which typically

operate with acquisition rates on the order of 1 Hz. Modern cameras can be equipped with electron multiplier modules that enable faster acquisition rate on the order of 100–1000 Hz. Examples of applications of these fast cameras to monitor transient processes in SERS have been reported.<sup>34</sup> On the other hand, point detectors, such as photomultiplier tubes and avalanche photodiodes, can provide much faster acquisition rates ( $\sim 1$  MHz) than a typical CCD camera. Furthermore, the use of point detector arrays enables fast imaging and the application of super-resolution techniques,<sup>35</sup> allowing the investigation of both the spatial distribution and fast time-dependent behavior of SERS events. The drawback of single point detectors for SERS investigations is the lack of spectral discrimination. This means that transient spectral signatures of carbonaceous materials and additional background from, for instance, plasmonic or molecular luminescence will be convoluted with the signal. However, as long as those side processes do not dominate the signal in the whole time-dependent data acquisition trajectory (i.e.; they are “transitory” events in the time scale of the whole experiment), they will be statistically insignificant. In that case, they represent a minority

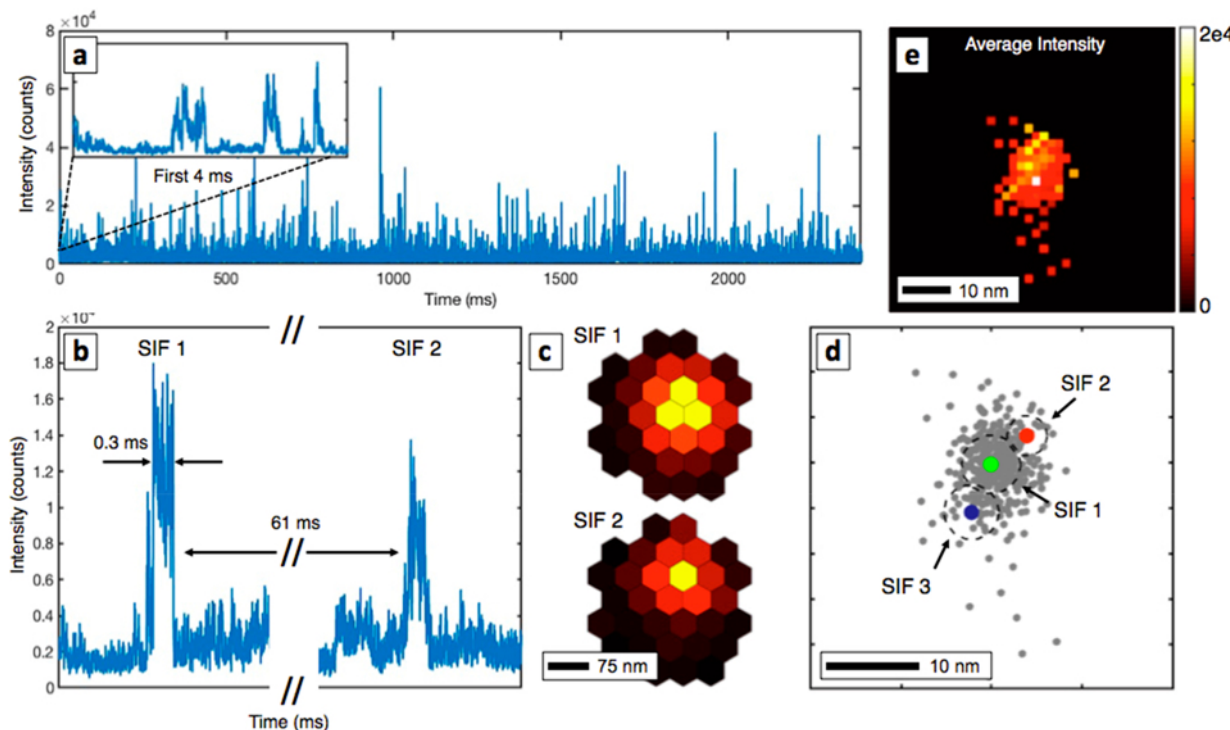


**Figure 4.** High-speed SERS signal acquisition and super-resolution imaging. (a) Typical SERS intensity fluctuation (SIF) time trajectory. Over several seconds, the signal has a large number of single SIFs that occur on the submillisecond time scale. The spectral range, determined by the filter set, here covered  $500\text{ cm}^{-1}$  to  $\sim 2000\text{ cm}^{-1}$ . (b) Zoomed-in view of two characteristic SIFs, lasting for  $\sim 0.3\text{ ms}$  each and occurring  $61\text{ ms}$  apart. (c) On the Airyscan detector, the point-spread-function of the emitted light can be imaged. The two SIFs are seen to originate from different locations on the single particle. (d) Over time, many SIFs can be accumulated and fit to eventually form an image of the particle (see comments about localization error in the main text). Three SIFs are shown here with the dashed line representing the standard deviation of the fit location over the multiple frames of the single SIF event. The gray dotted background shows the positions of all the SIF events over the course of several seconds. (e) An image of the average localized SERS intensity over the surface of the single nanoparticle. Figure adapted with permission from ref 14. Copyright 2019 Nature Publishing Group.

of events in a large data set. Other origins of spectral fluctuations, such as a molecule's orientation within a hotspot enhancing certain peaks over other peaks, would still be captured by a point detector as an event, but not fully characterized. Experimentally, many of these effects can be mitigated and verified by using band-pass filters that monitor the intensity fluctuations in spectral regions with no SERS activity or monitoring multiple peaks within the SERS spectrum.

Figure 3 shows an example of fast SERS imaging of single nanoshell nanoparticles in dry conditions performed using high speed laser rastering and collection on a single photomultiplier tube (PMT) point detector.<sup>13</sup> Figure 3a is a dark field hyperspectral image that was used to locate the individual particles dispersed on a glass slide. Figure 3b presents the plasmonic scattering profiles of three individual particles. The presence of dimers or large aggregates displayed a specific scattering signature (broad peaks with a long tail toward the red) and those types of structures were discarded. Figure 3c is an electron microscopy image of the nanoshells that demonstrates the presence of roughness features that enable localized plasmon effects at the particle surface. Figure 3d compares a SERS spectrum obtained in a regular Raman microscope (Renishaw inVia) with the spectrum obtained using the PMT by scanning a bandpass filter. Compared to a typical Raman spectrometer, the use of bandpass filters significantly reduces the spectral resolution. On the other hand, by collecting a broad region of the Stokes-shifted

spectrum, a larger number of photons are captured by the single point detector. This allows for fast imaging and the observation of dynamical SERS processes even from a fully coated nanoparticle.<sup>13</sup> SERS images of the nanoparticles are shown in Figure 3e. All SERS measurements were realized using low power excitation (typically less than  $100\text{ }\mu\text{W}/\mu\text{m}^2$ ) to avoid spurious artifacts due to photodecomposition. The images were recorded by laser scanning a  $\sim 4 \times 4\text{ }\mu\text{m}^2$  area of the surface at 200 frames per second ( $\sim 1.5\text{ }\mu\text{s}$  dwell time per pixel). The laser radiation was removed by a bandpass filter, and the Stokes-shifted photons were collected in the PMT. Strong SIFs, manifested by large change in brightness at the position of the nanoparticles, were observed between images obtained at 200 fps (Figure 3e). The observation of intensity fluctuations in the images was surprising because the surface was totally coated and these variations were absent when the experiments were realized using the longer exposure times typically used in SERS experiments ( $\sim 1\text{ s}$ ). The magnitude of the intensity fluctuations was quantified by recording the signal from a single pixel at the center of a single nanoparticle and plotting its variation against time. Figure 3f shows this SIF trajectory, and it clearly demonstrates that a significant amount of photons were generated from distinct events. Notice that in a regular Raman spectrometer those fluctuations would average out as the acquisition is done at a much larger time scale (1 Hz).

The fact that SIFs become more evident at higher acquisition rates, as shown in Figure 3, reveals a hidden

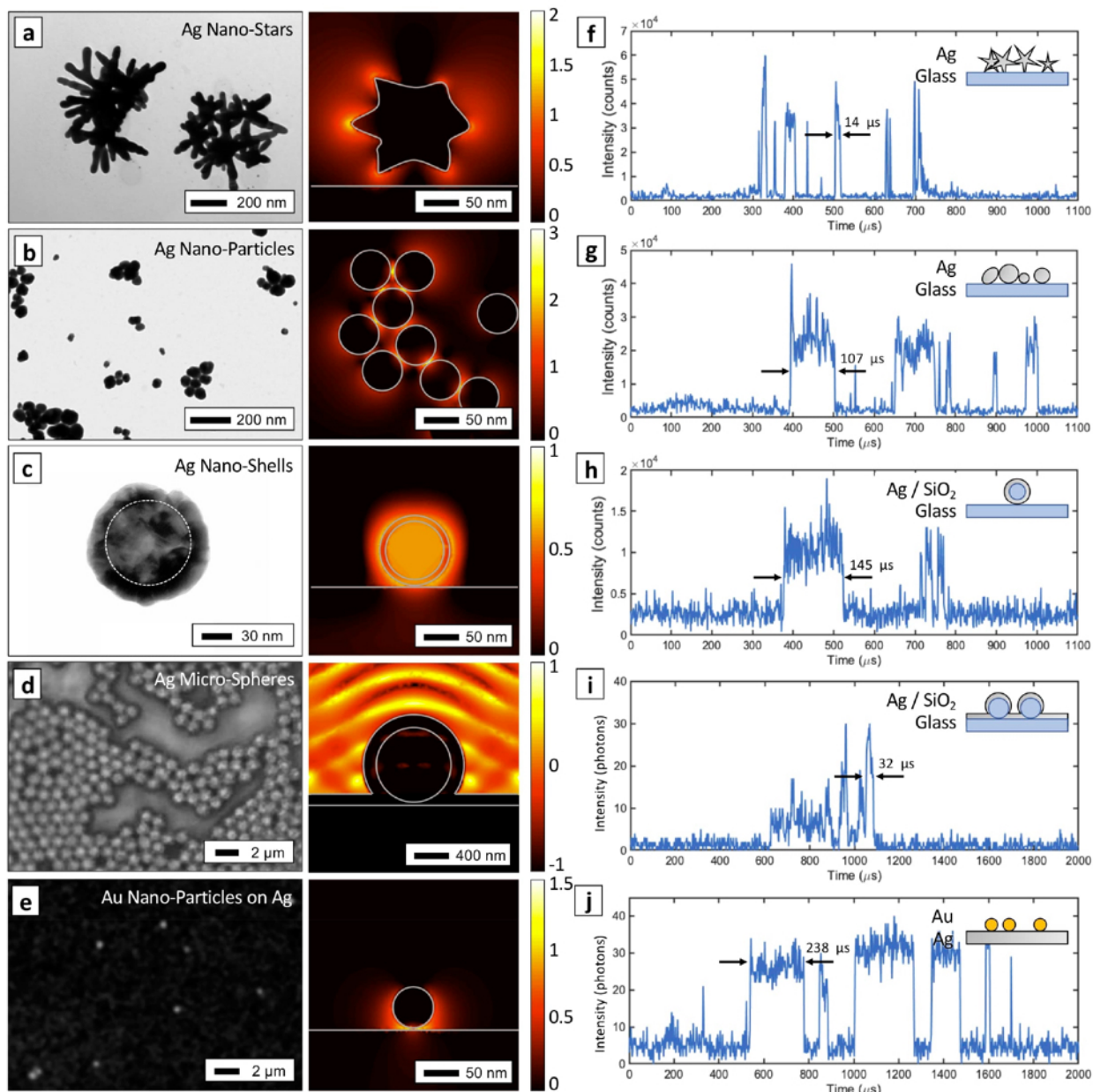


**Figure 5.** Various nanostructured systems show high-speed SERS intensity fluctuations obtained with 633 nm excitation: (a) TEM images of Ag nanostars; (b) TEM images of Ag nanoparticle clusters; (c) TEM images of Ag nanoshells. All structures in parts a–c were coated with DTNB for SERS measurements. (d) Optical microscope image of Ag-coated silica microspheres. (e) SEM image of Au nanoparticles on an Ag film. The structures in parts d and e were coated with benzenethiol molecules. Each image of the nanostructures in parts a–e are accompanied by COMSOL finite-element simulations of the electric field intensity. The calculations used qualitatively similar structures that were illuminated with a focused 633 nm beam. The results of the calculations are log-scale plots of the field amplitude normalized to the field amplitude without the nanostructure but with the substrate. (f–j) Time-series scans obtained using a high-speed point detector. Figure adapted with permission from ref 39. Copyright 2020 Society of Spectroscopy.

phenomenon in SERS and raises questions regarding the actual nature of the events that drive those fluctuations. In order to address those issues, single particle images under the same conditions as Figure 3 were acquired using even faster acquisition rates ( $\sim 1$  MHz). Parts a and b of Figure 4 present the time trajectory for the SERS intensities recorded at those ultrahigh speed acquisition rates. Figure 4 emphasizes that single events observed in the 100s of microseconds time scale are actually a series of fast dynamic events, lasting only a few microseconds each. Even more surprising is the realization that in SERS (at least for the experimental conditions of Figure 4)

very short bright events are followed by long periods of inactivity (see Figure 4b). In other words, the particle is “dark” most of the time. This is a phenomenon that has been hidden so far, because most SERS measurements are done with  $\sim 1$  s integration times, which average out those fast fluctuations. It is important to emphasize that the specific SIF behavior observed in Figure 4b, such as fluctuation rate and overall signal intensity, could be affected by experimental parameters, such as excitation energy, laser power, and the integration time. Beyond single point measurements, imaging at high speeds is also possible. While the frame rate (200 Hz) of the single

particle images in **Figure 3e** was obtained by scanning the excitation laser over the surface of the sample, a much faster acquisition rate was achieved in **Figure 4** by using a stationary laser beam coupled to an array of PMTs. This technology, illustrated in **Figure 4c**, allows direct imaging of the Airy region, or the width of the focused laser. Using centroid fitting techniques that are common in super-resolution fluorescence spectroscopy,<sup>10</sup> it is possible to determine the “position” of the single molecule scattered from a single particle in each given event. Since SIFs occur at very fast rates (see **Figure 4b**), it is then possible to spatially plot those centroid positions and generate an “image” from the scatters, as shown in parts d and e of **Figure 4**. This is akin to recording a “movie” of the SIF events at a million frames per second. However, it is very important to point out that the “images” in parts d and e of **Figure 4** are not a real geometric representation of the single particle. The scattering in SERS involves the molecule–metal system; therefore, the whole system affects the directionality of the emission.<sup>37,38</sup> In fact, the image centroid is expected to shift toward the geometric center of the nanoparticle. The result of this shift is that the SERS images presented in parts d and e of **Figure 4** are much smaller than the actual nanoparticle size of 100 nm, since they represent a convolution of the molecule–hotspot environments distributed throughout the single particle. **Figure 4d** shows the fitting results of three SIFs events, where the dashed circle is to illustrate the fitting variation. **Figure 4d** clearly illustrates that each of the three SIF events, despite the localization error discussed above, are well separated spatially, suggesting that they originate from different hotspots present in a single particle. The results from **Figure 4** also support the idea that single molecule SERS can be observed even from totally covered particles, as discussed in **Figure 1c**. In this case, the fast acquisition enables the observation of scattering only from the small number of molecules that, by chance, are present on highly efficient hotspots at a particular moment. These moments are incredibly fleeting, lasting just a few microseconds. The unique contributions from individual hotspots were further confirmed by simultaneously exciting the particle with two lasers with different energies, 543 nm (green) and 633 nm (red), and recording into two spectrally separated channels. In some occasions, the Stokes-shifted SIF activities were seen to originate from different locations at different times for each of the excitation colors. Similarly, experiments performed using two different polarizations (perpendicular to each other) also revealed selective excitation of different areas on a single particle,<sup>39</sup> suggesting that the excitation conditions for individual hotspot environments were accessed.

The statistics of the time dependent SIFs presented in **Figures 3** and **4** seems to imply that hotspots are turned on (and off) in very localized regions on the single nanoparticle, which allow single molecule events to be observed even from a fully coated surface. Similar behavior has been observed for different experimental conditions in the context of TERS and a NPoM geometry.<sup>24,40</sup> These suggest that the observed behavior might be a general characteristic of SERS and should be observed in a variety of nanostructured metallic environment, as long as the experimental acquisition rates are sufficiently fast. **Figure 5** presents results from SERS experiments at ultrahigh speed acquisition (800 kHz), as described in parts a and b of **Figure 4**, but for different nanoparticle shapes, materials, molecules, and conditions. The results in **Figure 5** suggest that the fast SIF phenomenon is indeed general in

SERS, since it is observed for single Ag particles of different particle shapes (**Figures 5**, parts a and c), from Ag nanoparticles clusters or coupled systems (**Figure 5**, parts b and d) and from Au nanoparticles. The intensity fluctuations also occur for different adsorbates (DTNB in **Figure 5a–c** and benzenethiol in **Figure 5**, parts d and e).

The time trajectories (**Figure 5f–j**) presented short-lived (a few microseconds) SERS events followed by periods of inactivity, in agreement with the observations from **Figure 4**, parts a and b. Histograms of the SERS active “ON”-time events and SERS inactive “OFF”-time events for all systems indicated in **Figure 5a–e** followed a log-normal distribution, similar to the shape represented schematically in **Figure 1b**. The mode of the distributions appeared in the  $\sim 100 \mu\text{s}$  region, and their long tails extended up to a few milliseconds. The common qualitative behavior suggests that the dynamics in all nanostructures were driven by the same phenomenon. Although the results from **Figure 5** presented variations between particles in the same system, a preliminary quantification assessment indicated some interesting revelations about the mechanism of processes at atomic level. For instance, a comparison between the time dependent behavior in **Figure 5** indicates that Ag nanostars (**Figure 5a**) supported shorter SIF events, on average, while the metallic aggregates in **Figure 5b** presented the larger frequency of events among all systems investigated. These observations are in accordance to the idea that the SIF events are driven by random atomic processes that enhance the local hotspot field in a region containing a small number of molecules. The localized hotspots in nanostars (**Figure 5a**) are mostly concentrated in the tips of the nanostructure, which are small areas of potentially high chemical activity. This should decrease the lifetime of highly transient localized hotspots. On the other hand, the electric field is more spread-out in metallic aggregates (**Figure 5b**), leading to larger density of hotspots and a higher probability of more SIF events per unit of time, each of them with relatively longer durations. For instance,  $\sim 25\%$  of the SIF events recorded from an Ag-coated microsphere (**Figure 5d**) were longer than 1 ms. Finally, a head-to-head comparison between single Au and single Au nanoparticles suggests differences in atomic/cluster mobility between the two metals, with Au showing a slightly longer SIF duration. These initial considerations are enticing and exciting, since they suggest that fundamental information on atomic and molecular mechanisms can be inferred from SIFs. Similar conclusions were achieved in a recent work involving a NPoM geometry coupled to a nanolens to enable 17  $\mu\text{s}$  time-resolved SERS measurements using an EM-CCD.<sup>33</sup> It is clear that more comprehensive investigations, using more statistically significant data sets, should follow all these preliminary ultrahigh speed SERS findings.

## ■ PERSPECTIVES FOR ULTRA-HIGH SPEED SERS MEASUREMENTS

Using ultrahigh speed SERS intensity fluctuations as a tool to study the dynamics of localized molecular and atomic processes is an exciting prospect. However, as is the case for most of the behavior observed in SERS, there are a variety of challenges and complications that must also be taken into consideration. First and foremost is the random nature of the hotspot conditions, which will require large data sets and robust approaches to support any quantitative and statistically significant findings.<sup>11,41</sup> The fact that some SERS particles are

“dark” nearly 98% of the time also necessitates long data acquisition times (minutes) with very high-speed detection rates (MHz) to capture a meaningful number of SIF events. This generates an enormous amount of data, with 10s or 100s of billions of data points. Furthermore, there are other sources of fluctuations that can either compete or convolute with the SERS response. For instance, metallic nanostructures and clusters might present intrinsic luminescence that can confound acquisitions using single point detectors without spectral discrimination (as in ref 14).<sup>42</sup> Photodecomposition of the molecular probe or stabilizers and coatings remaining from the nanoparticle synthesis can also provide spurious spectral changes including transient signatures of carbonaceous materials.<sup>43,44</sup> The physical chemical properties of these additional fluctuations are exciting on their own and require attention by the SERS research community. An example of an interesting “side-effect” phenomenon in this area is the case of strong fluctuations of the luminescent (broad) background that accompany SERS.<sup>45–47</sup> Fluctuations of this background, dubbed as “flares” in ref 48, can also be correlated to dynamic atomic cluster reconstructions, insinuating they have an origin similar to that of the fast SERS phenomenon. The inelastic electronic scattering that gives rise to these broad backgrounds in SERS leads to emissions that may cover both higher and lower energy ranges relative to the excitation laser. This means that the background sometimes span from the anti-Stokes to the Stokes side, enabling new approaches for thermometry.<sup>47</sup> On the other hand, the investigation of fast fluctuations of anti-Stokes to Stokes SERS (aS/S) ratio also opens the door to a variety of new physical insights. For instance, in contrast to normal Raman scattering, the aS/S ratio in SERS cannot be simply used for temperature measurements because the resonance conditions of the hotspots lead to extreme deviations from a simple Boltzmann behavior.<sup>49–51</sup> Extremely hot transitions, representing strong anti-Stokes peaks even at 1000s  $\text{cm}^{-1}$  away from the Rayleigh line, are observed under those resonance conditions in SERS and TERS.<sup>24</sup> The aS/S ratio has also been correlated to the phenomenon of vibrational pumping driven by the very strong electric field at the highly localized hotspot. Although the concept of vibrational pumping has been challenged,<sup>52,53</sup> it is conceivable that individual nonlinear effects, which are hidden in average behavior, might become more apparent when single molecule events are followed at high-speed in conditions of extreme localization.<sup>54</sup> The identification and exploration of the dynamics of these ultrahigh speed effects, including SIFs, background fluctuations, and aS/S ratio effects, provide a pathway for understanding nanoscopic processes such as atomic or cluster reconstruction. They may even constitute another frontier for exploration in SERS. Beyond the perspective of fundamentally new directions that can be revealed through the analysis of SIFs at high speed, there are also prospects for applications of SIFs in both analytical chemistry and chemical imaging. The understanding of plasmonic-induced fluctuations can allow for quantification at ultralow concentrations.<sup>55</sup> For instance, the recording of changes in fluctuation frequency, rather than absolute intensity, might help mitigate the other variations from substrate effects.<sup>41</sup> Super-resolution fluorescence has led to a revolution in biological imaging<sup>56</sup> and will continue to drive discoveries in SERS.<sup>57</sup> SIFs can be explored for the implementation of methods that rely on time dependent intensity variations,

analogous to stochastic optical reconstruction microscopy (STORM),<sup>58</sup> to image dynamic events even in a single cell.<sup>59,60</sup>

Historically, SERS is a field that refuses to die. There have been several periods when the field was believed to be exhausted, but there have always been new physics, experimental challenges, and tantalizing applications that kept the interest of a large number of researchers. The renaissance of SERS due to single molecule detection in the late 1990s has accelerated along with advances in nanofabrication, synthesis, optical measurements and computational methods in the last few decades. We are perhaps now witnessing another defining moment in this area, powered by very exciting findings, such as incredible improvements in spatial resolution in TERS that allow the imaging of single vibrational modes.<sup>61</sup> The exploration of effects at the highest temporal and spatial resolutions discussed here provides yet another and virtually uncharted area in SERS. The potential for new discoveries by exploring the new effects revealed by fast measurements could become the next frontier in SERS.

## ■ AUTHOR INFORMATION

### Corresponding Author

Alexandre G. Brolo — *Department of Chemistry and Center for Advanced Materials and Related Technologies (CAMTEC), University of Victoria, Victoria, BC V8P 5C2, Canada; [orcid.org/0000-0002-3162-0881](https://orcid.org/0000-0002-3162-0881); Email: [agbrolo@uvic.ca](mailto:agbrolo@uvic.ca)*

### Author

Nathan C. Lindquist — *Department of Physics and Engineering, Bethel University, Saint Paul, Minnesota 55112, United States; [orcid.org/0000-0002-1226-5212](https://orcid.org/0000-0002-1226-5212)*

Complete contact information is available at: <https://pubs.acs.org/10.1021/acs.jpcc.0c11150>

### Notes

The authors declare no competing financial interest.

### Biographies



Dr. Nathan C. Lindquist received his Ph.D. in Electrical Engineering from the University of Minnesota and is a Professor of Physics and Engineering at Bethel University in St. Paul, Minnesota, United States. His research interests include interdisciplinary applied optics, holography, nanophotonics, and surface-enhanced Raman spectroscopy. Recently Dr. Lindquist and his undergraduate research students at Bethel have been developing new techniques for optical tweezing and super-resolution imaging using plasmonic nanoparticles.



Photo by Jasspreet Sahib.

Dr. Alexandre G. Brolo is Professor of Chemistry at the University of Victoria in British Columbia, Canada. He obtained his M.Sc. from the University of São Paulo (Brazil) and his Ph.D. from the University of Waterloo (Canada). Dr. Brolo's research interests are the fabrication of nanostructured metal surfaces, the investigation of their optical properties, and their application in analytical chemistry. He is well-known for his work on the development of new types of surface plasmon resonance sensors and in the field of surface-enhanced spectroscopy, particularly on surface-enhanced Raman scattering (SERS).

## ACKNOWLEDGMENTS

N.C.L. acknowledges support from the National Science Foundation (NSF), Awards 1552642 and 2003750. The work in A.G.B.'s lab is supported by operational grants from the Natural Sciences and Engineering Research Council of Canada (NSERC) and instrument grants by the Canada Foundation for Innovation (CFI), the British Columbia Knowledge Development Fund (BCKDF), and the University of Victoria.

## REFERENCES

- (1) Langer, J.; Jimenez de Aberasturi, D.; Aizpurua, J.; Alvarez-Puebla, R. A.; Auguié, B.; Baumberg, J. J.; Bazan, J. C.; Bell, S. E. J.; Boisen, A.; Brolo, A. G.; et al. Present and Future of Surface-Enhanced Raman Scattering. *ACS Nano* **2020**, *14*, 28–117.
- (2) Ding, S. Y.; You, E. M.; Tian, Z. Q.; Moskovits, M. Electromagnetic Theories of Surface-Enhanced Raman Spectroscopy. *Chem. Soc. Rev.* **2017**, *46*, 4042–4076.
- (3) Fan, M.; Andrade, G. F. S.; Brolo, A. G. A Review on the Fabrication of Substrates for Surface Enhanced Raman Spectroscopy and Their Applications in Analytical Chemistry. *Anal. Chim. Acta* **2011**, *693*, 7–25.
- (4) Fan, M. K.; Andrade, G. F. S.; Brolo, A. G. A Review on Recent Advances in the Applications of Surface-Enhanced Raman Scattering in Analytical Chemistry. *Anal. Chim. Acta* **2020**, *1097*, 1–29.
- (5) Perez-Jimenez, A. I.; Lyu, D.; Lu, Z. X.; Liu, G. K.; Ren, R. B. Surface-Enhanced Raman Spectroscopy: Benefits, Trade-Offs and Future Developments. *Chemical Science* **2020**, *11*, 4563–4577.
- (6) dos Santos, D. P.; Temperini, M. L. A.; Brolo, A. G. Intensity Fluctuations in Single-Molecule Surface-Enhanced Raman Scattering. *Acc. Chem. Res.* **2019**, *52*, 456–464.
- (7) Wrzosek, B.; Kitahama, Y.; Ozaki, Y. Sers Blinking on Anisotropic Nanoparticles. *J. Phys. Chem. C* **2020**, *124*, 20328–20339.
- (8) Yamamoto, Y. S.; Ishikawa, M.; Ozaki, Y.; Itoh, T. Fundamental Studies on Enhancement and Blinking Mechanism of Surface-Enhanced Raman Scattering (Sers) and Basic Applications of Sers Biological Sensing. *Frontiers of Physics* **2014**, *9*, 31–46.
- (9) Emory, S. R.; Jensen, R. A.; Wenda, T.; Han, M. Y.; Nie, S. M. Re-Examining the Origins of Spectral Blinking in Single-Molecule and Single-Nanoparticle Sers. *Faraday Discuss.* **2006**, *132*, 249–259.
- (10) Miller, H.; Zhou, Z. K.; Shepherd, J.; Wollman, A. J. M.; Leake, M. C. Single-Molecule Techniques in Biophysics: A Review of the Progress in Methods and Applications. *Rep. Prog. Phys.* **2018**, *81*, 024601.
- (11) Margueritat, J.; Bouhelier, A.; Markey, L.; Colas des Francs, G. C.; Dereux, A.; Lau-Truong, S.; Grand, J.; Lévi, G.; Félidj, N.; Aubard, J.; et al. Discerning the Origins of the Amplitude Fluctuations in Dynamic Raman Nanospectroscopy. *J. Phys. Chem. C* **2012**, *116*, 26919–26923.
- (12) Chikkaraddy, R.; de Nijs, B.; Benz, F.; Barrow, S. J.; Scherman, O. A.; Rosta, E.; Demetriadou, A.; Fox, P.; Hess, O.; Baumberg, J. J. Single-Molecule Strong Coupling at Room Temperature in Plasmonic Nanocavities. *Nature* **2016**, *535*, 127–130.
- (13) de Albuquerque, C. D. L.; Hokanson, K. M.; Thorud, S. R.; Sobral-Filho, R. G.; Lindquist, N. C.; Brolo, A. G. Dynamic Imaging of Multiple Sers Hotspots on Single Nanoparticles. *ACS Photonics* **2020**, *7*, 434–443.
- (14) Lindquist, N. C.; de Albuquerque, C. D. L.; Sobral-Filho, R. G.; Paci, I.; Brolo, A. G. High-Speed Imaging of Surface-Enhanced Raman Scattering Fluctuations from Individual Nanoparticles. *Nat. Nanotechnol.* **2019**, *14*, 981–987.
- (15) Lombardi, J. R.; Birke, R. L.; Haran, G. Single Molecule Sers Spectral Blinking and Vibronic Coupling. *J. Phys. Chem. C* **2011**, *115*, 4540–4545.
- (16) Otto, A. Theory of First Layer and Single Molecule Surface Enhanced Raman Scattering (Sers). *Physica Status Solidi a-Applications and Materials Science* **2001**, *188*, 1455–1470.
- (17) Lombardi, J. R.; Birke, R. L. A Unified View of Surface-Enhanced Raman Scattering. *Acc. Chem. Res.* **2009**, *42*, 734–742.
- (18) Yang, L. L.; Peng, Y. S.; Yang, Y.; Liu, J. J.; Huang, H. L.; Yu, B. H.; Zhao, J. M.; Lu, Y. L.; Huang, Z. R.; Li, Z. Y. A Novel Ultra-Sensitive Semiconductor Sers Substrate Boosted by the Coupled Resonance Effect. *Advanced Science* **2019**, *6*, 1900310.
- (19) Shi, H. T.; Zhao, B. F.; Ma, J.; Bronson, M. J.; Cai, Z.; Chen, J. H.; Wang, Y.; Cronin, M.; Jensen, L.; Cronin, S. B. Measuring Local Electric Fields and Local Charge Densities at Electrode Surfaces Using Graphene-Enhanced Raman Spectroscopy (Gers)-Based Stark-Shifts. *ACS Appl. Mater. Interfaces* **2019**, *11*, 36252–36258.
- (20) Kelly, K. L.; Coronado, E.; Zhao, L. L.; Schatz, G. C. The Optical Properties of Metal Nanoparticles: The Influence of Size, Shape, and Dielectric Environment. *J. Phys. Chem. B* **2003**, *107*, 668–677.
- (21) Hao, E.; Schatz, G. C. Electromagnetic Fields around Silver Nanoparticles and Dimers. *J. Chem. Phys.* **2004**, *120*, 357–366.
- (22) Markel, V. A.; Shalaev, V. M.; Zhang, P.; Huynh, W.; Tay, L.; Haslett, T. L.; Moskovits, M. Near-Field Optical Spectroscopy of Individual Surface-Plasmon Modes in Colloid Clusters. *Phys. Rev. B: Condens. Matter Mater. Phys.* **1999**, *59*, 10903–10909.
- (23) Fang, Y.; Seong, N.-H.; Dlott, D. D. Measurement of the Distribution of Site Enhancements in Surface-Enhanced Raman Scattering. *Science* **2008**, *321*, 388–392.
- (24) Richard-Lacroix, M.; Deckert, V. Direct Molecular-Level near-Field Plasmon and Temperature Assessment in a Single Plasmonic Hotspot. *Light: Sci. Appl.* **2020**, *9*, 35.
- (25) Benz, F.; Schmidt, M. K.; Dreismann, A.; Chikkaraddy, R.; Zhang, Y.; Demetriadou, A.; Carnegie, C.; Ohadi, H.; de Nijs, B.; Esteban, R.; et al. Single-Molecule Optomechanics in "Picocavities". *Science* **2016**, *354*, 726–729.
- (26) Shin, H.-H.; Yeon, G. J.; Choi, H.-K.; Park, S.-M.; Lee, K. S.; Kim, Z. H. Frequency-Domain Proof of the Existence of Atomic-Scale Sers Hot-Spots. *Nano Lett.* **2018**, *18*, 262–271.
- (27) Zrimsek, A. B.; Wong, N. L.; Van Duyne, R. P. Single Molecule Surface-Enhanced Raman Spectroscopy: A Critical Analysis of the Bimolecular Versus Isotopologue Proof. *J. Phys. Chem. C* **2016**, *120*, 5133–5142.

(28) dos Santos, D. P.; Andrade, G. F. S.; Temperini, M. L. A.; Brolo, A. G. Electrochemical Control of the Time-Dependent Intensity Fluctuations in Surface-Enhanced Raman Scattering (Sers). *J. Phys. Chem. C* **2009**, *113*, 17737–17744.

(29) Kiefl, E. J.; Kiefl, R. F.; dos Santos, D. P.; Brolo, A. G. Evaluation of Surface-Enhanced Raman Spectroscopy Substrates from Single-Molecule Statistics. *J. Phys. Chem. C* **2017**, *121*, 25487–25493.

(30) Wang, Z. J.; Rothberg, L. J. Origins of Blinking in Single-Molecule Raman Spectroscopy. *J. Phys. Chem. B* **2005**, *109*, 3387–3391.

(31) Kitahama, Y.; Enogaki, A.; Tanaka, Y.; Itoh, T.; Ozaki, Y. Truncated Power Law Analysis of Blinking Sers of Thiacyanine Molecules Adsorbed on Single Silver Nanoaggregates by Excitation at Various Wavelengths. *J. Phys. Chem. C* **2013**, *117*, 9397–9403.

(32) Readman, C.; de Nijs, B.; Szabo, I.; Demetriadou, A.; Greenhalgh, R.; Durkan, C.; Rosta, E.; Scherman, O. A.; Baumberg, J. J. Anomalously Large Spectral Shifts near the Quantum Tunnelling Limit in Plasmonic Rulers with Subatomic Resolution. *Nano Lett.* **2019**, *19*, 2051–2058.

(33) Kamp, M.; de Nijs, B.; Kongsuwan, N.; Saba, M.; Chikkaraddy, R.; Readman, C. A.; Deacon, W. M.; Griffiths, J.; Barrow, S. J.; Ojambati, O. S.; et al. Cascaded Nanooptics to Probe Microsecond Atomic-Scale Phenomena. *Proc. Natl. Acad. Sci. U. S. A.* **2020**, *117*, 14819–14826.

(34) Zong, C.; Chen, C. J.; Zhang, M.; Wu, D. Y.; Ren, B. Transient Electrochemical Surface-Enhanced Raman Spectroscopy: A Millisecond Time-Resolved Study of an Electrochemical Redox Process. *J. Am. Chem. Soc.* **2015**, *137*, 11768–11774.

(35) Willets, K. A. Super-Resolution Imaging of Sers Hot Spots. *Chem. Soc. Rev.* **2014**, *43*, 3854–3864.

(36) Sobral-Filho, R. G.; Brito-Silva, A. M.; Isabelle, M.; Jirasek, A.; Lum, J. J.; Brolo, A. G. Plasmonic Labeling of Subcellular Compartments in Cancer Cells: Multiplexing with Fine-Tuned Gold and Silver Nanoshells. *Chemical Science* **2017**, *8*, 3038–3046.

(37) Heaps, C. W.; Schatz, G. C. Modeling Super-Resolution Sers Using a T-Matrix Method to Elucidate Molecule-Nanoparticle Coupling and the Origins of Localization Errors. *J. Chem. Phys.* **2017**, *146*, 224201.

(38) Goldwyn, H. J.; Smith, K. C.; Busche, J. A.; Masiello, D. J. Mislocalization in Plasmon-Enhanced Single-Molecule Fluorescence Microscopy as a Dynamical Young's Interferometer. *ACS Photonics* **2018**, *5*, 3141–3151.

(39) Bido, A. T.; Nordberg, B. G.; Engevik, M. A.; Lindquist, N. C.; Brolo, A. G. High-Speed Fluctuations in Surface-Enhanced Raman Scattering Intensities from Various Nanostructures. *Appl. Spectrosc.* **2020**, *74*, 1398.

(40) de Nijs, B.; Benz, F.; Barrow, S. J.; Sigle, D. O.; Chikkaraddy, R.; Palma, A.; Carnegie, C.; Kamp, M.; Sundararaman, R.; Narang, P. Plasmonic Tunnel Junctions for Single-Molecule Redox Chemistry. *Nat. Commun.* **2017**, *8*, 994.

(41) Brule, T.; Bouhelier, A.; Yockell-Lelievre, H.; Clement, J. E.; Leray, A.; Dereux, A.; Finot, E. Statistical and Fourier Analysis for in-Line Concentration Sensitivity in Single Molecule Dynamic-Sers. *ACS Photonics* **2015**, *2*, 1266–1271.

(42) Kitahama, Y.; Nagahiro, T.; Tanaka, Y.; Itoh, T.; Ozaki, Y. Analysis of Blinking from Multicoloured Sers-Active Ag Colloidal Nanoaggregates with Poly-L-Lysine Via Truncated Power Law. *J. Raman Spectrosc.* **2017**, *48*, 570–577.

(43) Kudelski, A. Some Aspects of Sers Temporal Fluctuations: Analysis of the Most Intense Spectra of Hydrogenated Amorphous Carbon Deposited on Silver. *J. Raman Spectrosc.* **2007**, *38*, 1494–1499.

(44) Pieczonka, N. P. W.; Aroca, R. F. Single Molecule Analysis by Surface-Enhanced Raman Scattering. *Chem. Soc. Rev.* **2008**, *37*, 946–954.

(45) Dvoynenko, M. M.; Wang, H. H.; Hsiao, H. H.; Wang, Y. L.; Wang, J. K. Study of Signal-to-Background Ratio of Surface-Enhanced Raman Scattering: Dependences on Excitation Wavelength and Hot-Spot Gap. *J. Phys. Chem. C* **2017**, *121*, 26438–26445.

(46) Mahajan, S.; Cole, R. M.; Speed, J. D.; Pelfrey, S. H.; Russell, A. E.; Bartlett, P. N.; Barnett, S. M.; Baumberg, J. J. Understanding the Surface-Enhanced Raman Spectroscopy "Background". *J. Phys. Chem. C* **2010**, *114*, 7242–7250.

(47) Hugall, J. T.; Baumberg, J. J. Demonstrating Photoluminescence from Au ls Electronic Inelastic Light Scattering of a Plasmonic Metal: The Origin of Sers Backgrounds. *Nano Lett.* **2015**, *15*, 2600–2604.

(48) Carnegie, C.; Urieta, M.; Chikkaraddy, R.; de Nijs, B.; Griffiths, J.; Deacon, W. M.; Kamp, M.; Zabala, N.; Aizpurua, J.; Baumberg, J. J. Flickering Nanometre-Scale Disorder in a Crystal Lattice Tracked by Plasmonic Flare Light Emission. *Nat. Commun.* **2020**, *11*, 682.

(49) Pozzi, E. A.; Zrimsek, A. B.; Lethiec, C. M.; Schatz, G. C.; Hersam, M. C.; Van Duyne, R. P. Evaluating Single-Molecule Stokes and Anti-Stokes Sers for Nanoscale Thermometry. *J. Phys. Chem. C* **2015**, *119*, 21116–21124.

(50) dos Santos, D. P.; Temperini, M. L. A.; Brolo, A. G. Mapping the Energy Distribution of Sers Hot Spots from Anti-Stokes to Stokes Intensity Ratios. *J. Am. Chem. Soc.* **2012**, *134*, 13492–13500.

(51) Brolo, A. G.; Sanderson, A. C.; Smith, A. P. Ratio of the Surface-Enhanced Anti-Stokes Scattering to the Surface-Enhanced Stokes-Raman Scattering for Molecules Adsorbed on a Silver Electrode. *Phys. Rev. B: Condens. Matter Mater. Phys.* **2004**, *69*, 045424.

(52) Le Ru, E. C.; Etchegoin, P. G. Vibrational Pumping and Heating under Sers Conditions: Fact or Myth? *Faraday Discuss.* **2006**, *132*, 63–75.

(53) Galloway, C. M.; Le Ru, E. C.; Etchegoin, P. G. Single-Molecule Vibrational Pumping in Sers. *Phys. Chem. Chem. Phys.* **2009**, *11*, 7372–7380.

(54) Schmidt, M. K.; Esteban, R.; González-Tudela, A.; Giedke, G.; Aizpurua, J. Quantum Mechanical Description of Raman Scattering from Molecules in Plasmonic Cavities. *ACS Nano* **2016**, *10*, 6291–6298.

(55) de Albuquerque, C. D. L.; Sobral-Filho, R. G.; Poppi, R. J.; Brolo, A. G. Digital Protocol for Chemical Analysis at Ultralow Concentrations by Surface-Enhanced Raman Scattering. *Anal. Chem.* **2018**, *90*, 1248–1254.

(56) Moerner, W. E.; Fromm, D. P. Methods of Single-Molecule Fluorescence Spectroscopy and Microscopy. *Rev. Sci. Instrum.* **2003**, *74*, 3597–3619.

(57) Willets, K. A.; Wilson, A. J.; Sundaresan, V.; Joshi, P. B. Super-Resolution Imaging and Plasmonics. *Chem. Rev.* **2017**, *117*, 7538–7582.

(58) Olson, A. P.; Spies, K. B.; Browning, A. C.; Soneral, P. A. G.; Lindquist, N. C. Chemically Imaging Bacteria with Super-Resolution Sers on Ultra-Thin Silver Substrates. *Sci. Rep.* **2017**, *7*, 9135.

(59) Olson, A. P.; Ertsgaard, C. T.; Elliott, S. N.; Lindquist, N. C. Super-Resolution Chemical Imaging with Plasmonic Substrates. *ACS Photonics* **2016**, *3*, 329–336.

(60) de Albuquerque, C. D. L.; Schultz, Z. D. Super-Resolution Surface-Enhanced Raman Scattering Imaging of Single Particles in Cells. *Anal. Chem.* **2020**, *92*, 9389–9398.

(61) Lee, J.; Crampton, K. T.; Tallarida, N.; Apkarian, V. A. Visualizing Vibrational Normal Modes of a Single Molecule with Atomically Confined Light. *Nature* **2019**, *568*, 78.